Supplementary Material

Effect of sodium doping on crystal growth and band matching of heterojunction in flexible CZTS solar cells

Qichen Zhao [a], Honglie Shen [a,b,*], Kai Gao [a], Yajun Xu [a], Xuewen Wang [a], Yufang Li [a]

[a] College of Science, Jiangsu Key Laboratory of Materials and Technology for Energy Conversion, Nanjing University of Aeronautics and Astronautics, Nanjing, 210016, PR China

[b] Jiangsu Collaborative Innovation Center of Photovoltaic Science and Engineering, Changzhou University, Changzhou, 213164, PR China

Tel/Fax: +86-25-52112626

Address: 29 Jiangjun Ave., 211100, Nanjing, China

1. Experimental detail

A clear yellow precursor solution was obtained by dissolving 0.958 g $Cu(CH_3COO)_2 \cdot H_2O$ (4.8 mmol), 0.724 g $Zn(CH_3COO)_2 \cdot 2H_2O$ (3.3 mmol), 0.745 g $SnCl_2 \cdot 2H_2O$ (3.3 mmol) and 1.979 g CH_4N_2S (26 mmol) into a solvent mixture of 10 mL dimethylformamide (DMF, AR) and 1mL Ethyl acetate (EA, AR). Subsequently, the precursor solution was spin-coated onto the flexible Mo-sputtered Ti substrates at

* Corresponding author: Jiangsu Key Laboratory of Materials and Technology for Energy Conversion, College of Materials Science and Technology, Nanjing University of Aeronautics and Astronautics, Nanjing, 210016, China
Email address: hlshen@nuaa.edu.cn

4600 rpm for 20 s. The sample was dried on a hot plate at 300 °C for 6 min in the air. This spin-coating process was repeated 15 times to obtain CZTS precursor films. For Na doping post-treatment, 0.05 mmol/mL NaCl, 0.05 mmol/mL CH_3COONa, and 0.025/0.05/0.1 mmol/mL $Na_2S_2O_3$ solutions were introduced as sodium sources, which were drip-coated on the surface of CZTS precursor films, followed by an annealing process on 60 °C on a hot plate for 10 min. All chemical reagents were purchased from Aladdin Reagent Co., Ltd. Fig. 1 depicts the process of sodium incorporation post-treatment toward CZTS precursor films.

2. Results and discussions

The crystal quality of absorber after sodium doping can also be determined by calculating the crystalline size, which can be obtained from Scherer formula $D=K\lambda/(\beta\cos\theta)$, where D is the crystalline size, K is the constant (0.89), λ is the X-ray wavelength (1.54 Å) and β is the FWHM of (112) peak. According to the information extracted from XRD, the detailed crystalline sizes of CZTS thin films are summarized in Table S1. Obviously, the calculated crystalline size of the absorber shows an increasing trend from 36.65 nm to 53.55nm, which indicates an improvement in crystal quality after sodium doping treatment.

Table S1. Detailed crystalline size of CZTS thin films.

	K	λ (Å)	β	θ (°)	D (nm)
No doping	0.89	1.54	$4.26\cdot10^{-3}$	28.53	36.65
NaCl	0.89	1.54	$3.15\cdot10^{-3}$	28.47	49.66
CH_3COONa	0.89	1.54	$3.57\cdot10^{-3}$	28.49	43.79
$Na_2S_2O_3$	0.89	1.54	$2.91\cdot10^{-3}$	28.46	53.55

In Fig. S1-S3, we obtained narrow scan spectra of the core energy levels of the metal elements in the precursor films. It is seen from Fig. S1 that the values of the binding energy of Cu 2p were 931.6 and 951.5 eV, and the splitting value of spin-

orbit (Δ_s) was 19.9 eV. Meanwhile, no satellite peak was observed at a higher binding energy position, indicating that there is only the +1 chemical state of Cu existing in samples. In Fig. S2, the values of the binding energy of Zn 2p were 1021.5 and 1044.5 eV, along with a Δ_s of 23.0 eV that corresponds to Zn (+2). From Fig. S3, it can be seen that the values of the binding energy of Sn 3d were 486.5 and 494.9eV, and the Δ_s was 8.4eV, indicating that there exists Sn (+4) in samples.

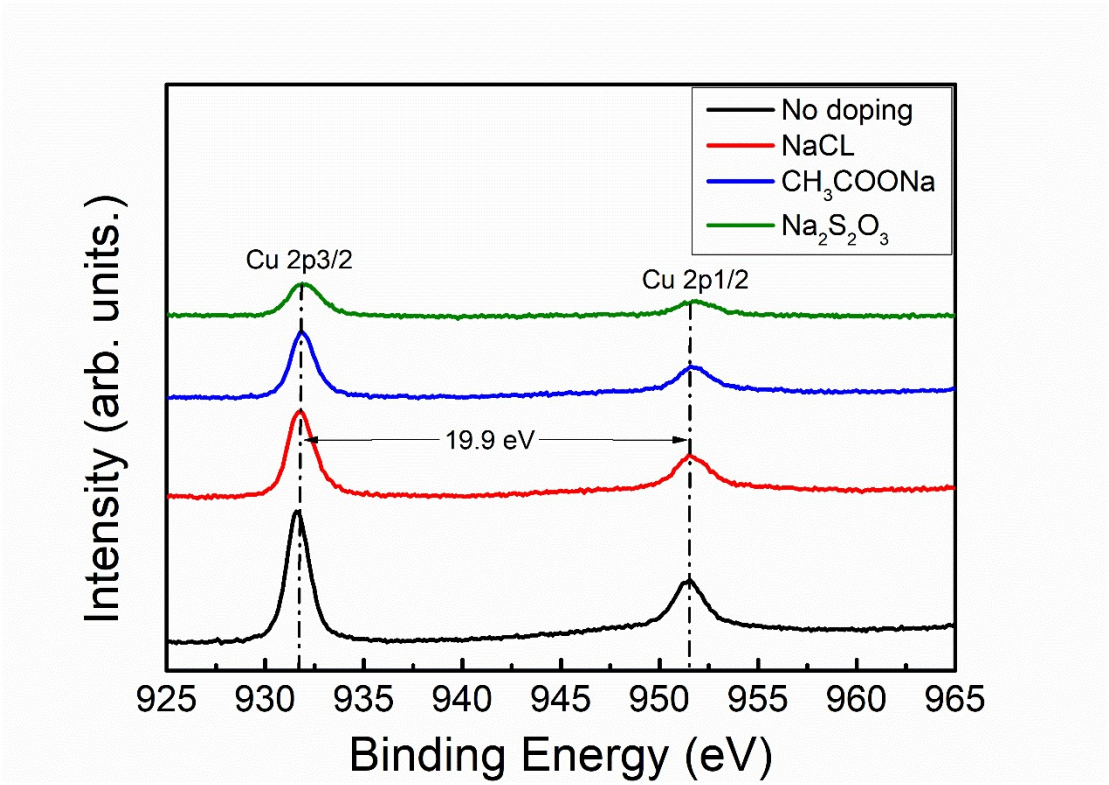

Fig. S1. XPS narrow scan spectra of the core levels of Cu 2p in precursor films.

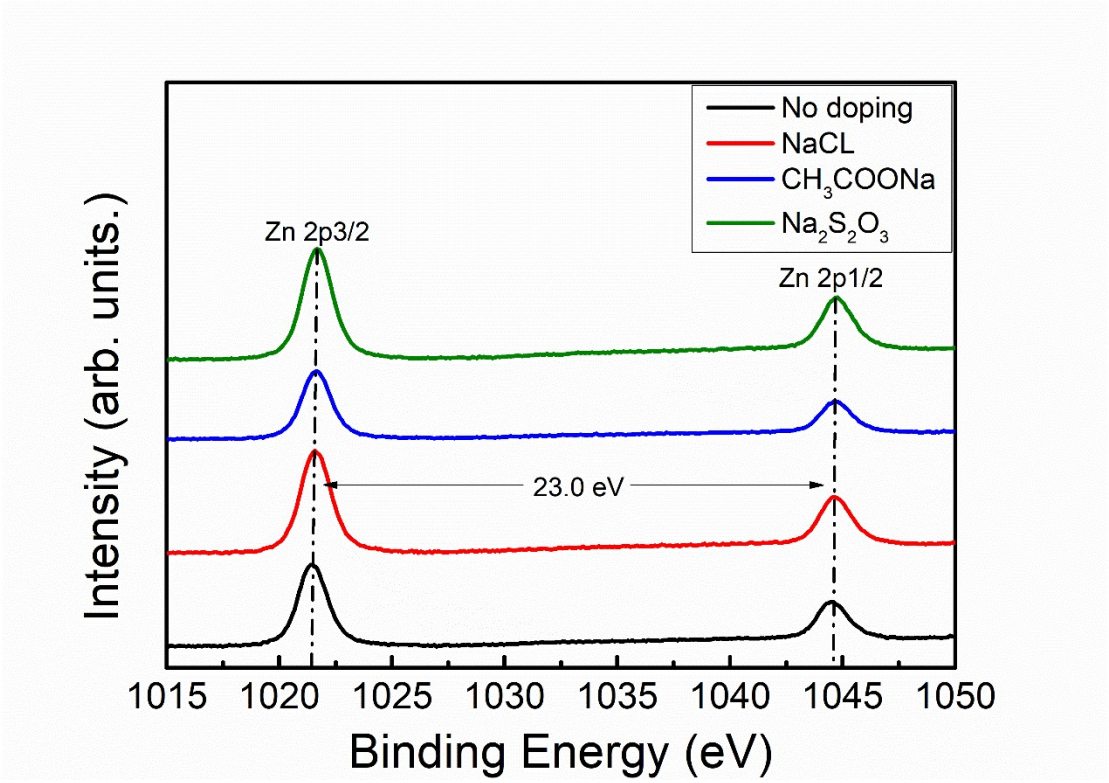

Fig. S2. XPS narrow scan spectra of the core levels of Zn 2p in precursor films.

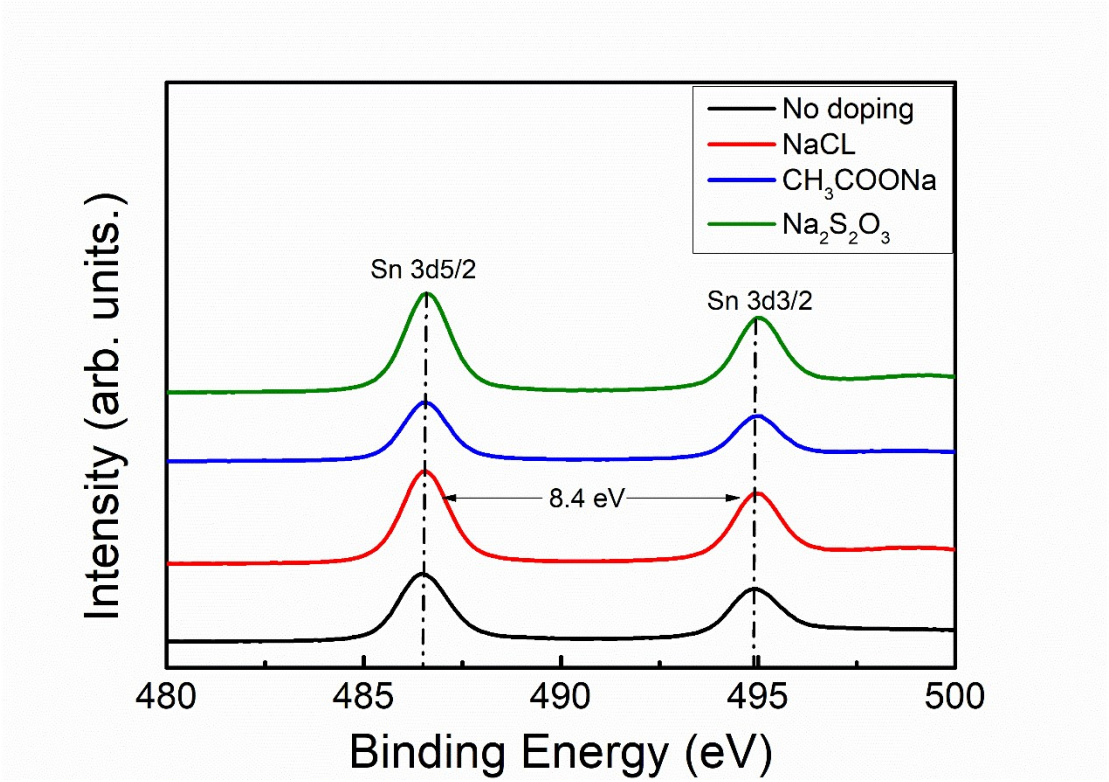

Fig. S3. XPS narrow scan spectra of the core levels of Sn 3d in precursor films.

In Fig. S4-S6, we obtained narrow scan spectra of core energy levels of metallic elements in films. As can be displayed, the visible peaks have binding energy positions of 932.1 eV (2p3/2) and 951.9 eV (2p1/2), 1021.8 eV (2p3/2) and 1044.7 eV (2p1/2) as well as 486.2 eV (3d5/2) and 494.5 eV (3d3/2), with corresponding spin-orbit splitting values (Δs) of 19.8 eV, 22.9 eV and 8.3 eV, respectively. Combined with the results of previous studies, we have confirmed that the ionic valence states of Cu, Zn, and Sn metal elements in the obtained films are +1, +2, and +4, respectively.

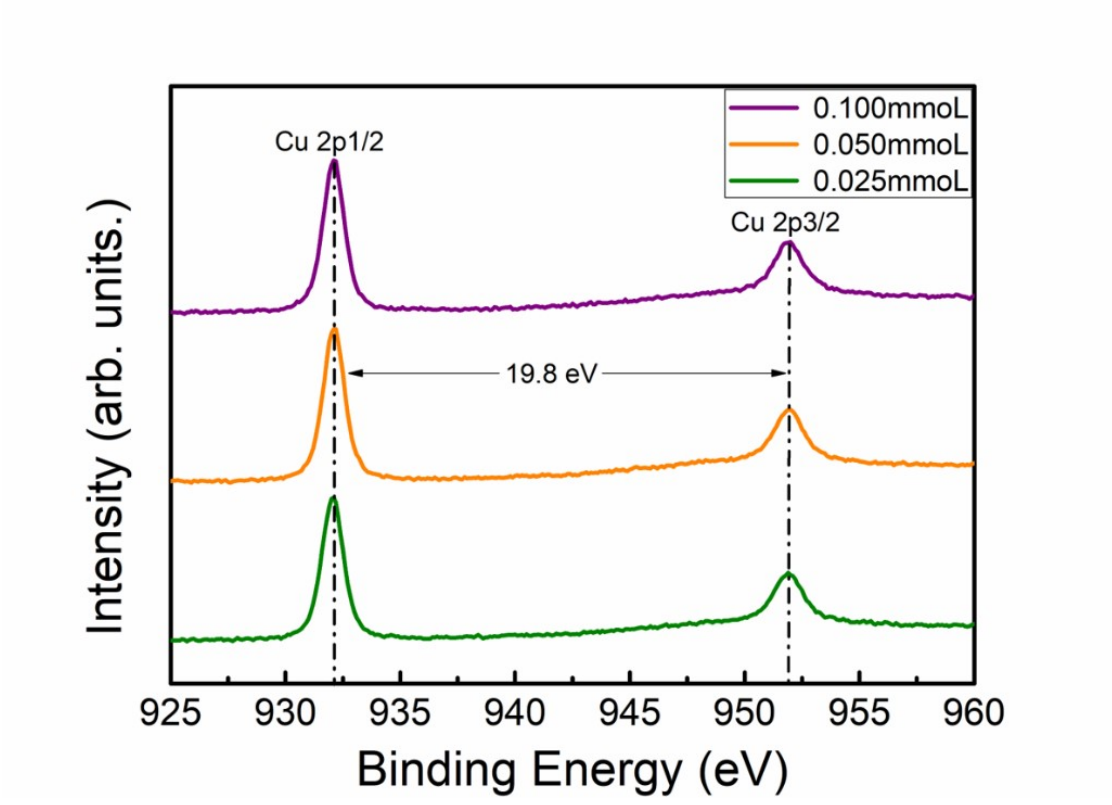

Fig. S4. XPS narrow scan spectra of the core levels of Cu 2p in CZTS films.

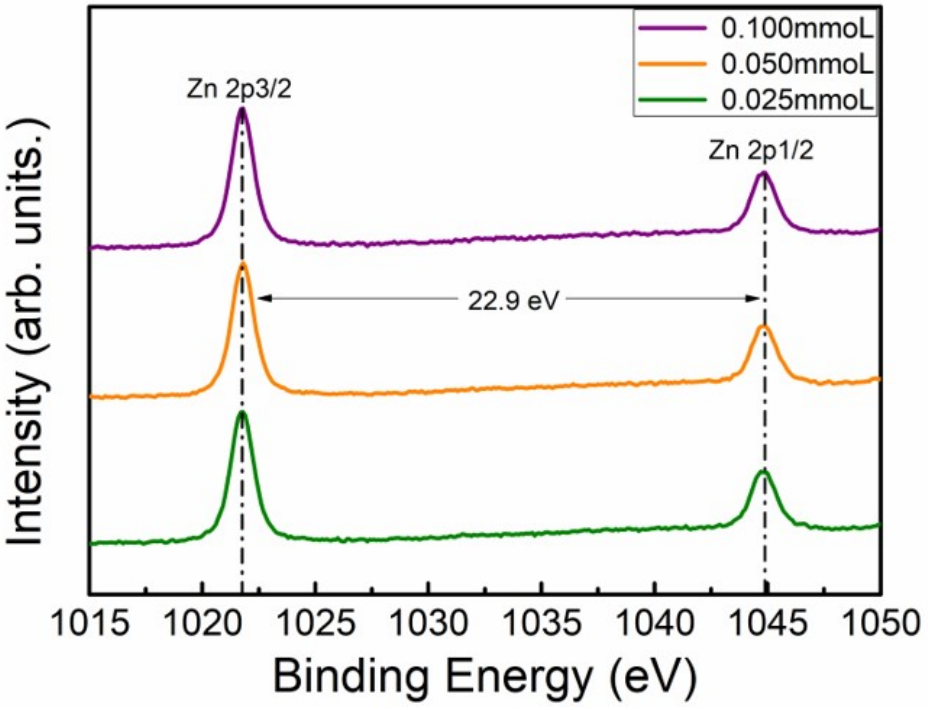

Fig. S5. XPS narrow scan spectra of the core levels of Zn 2p in CZTS films.

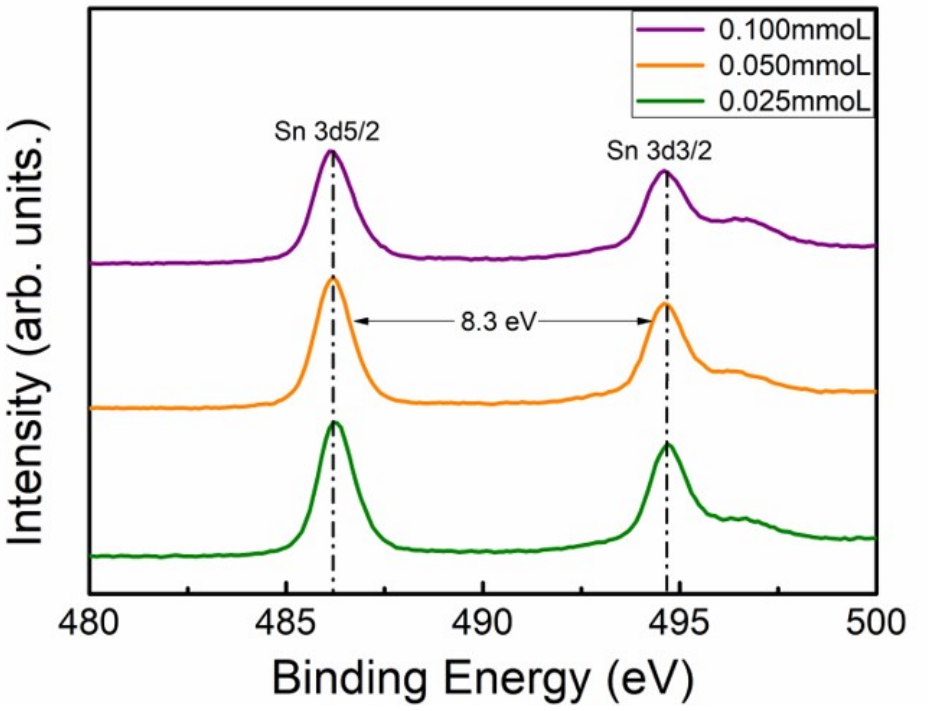

Fig. S6. XPS narrow scan spectra of the core levels of Sn 3d in CZTS films.

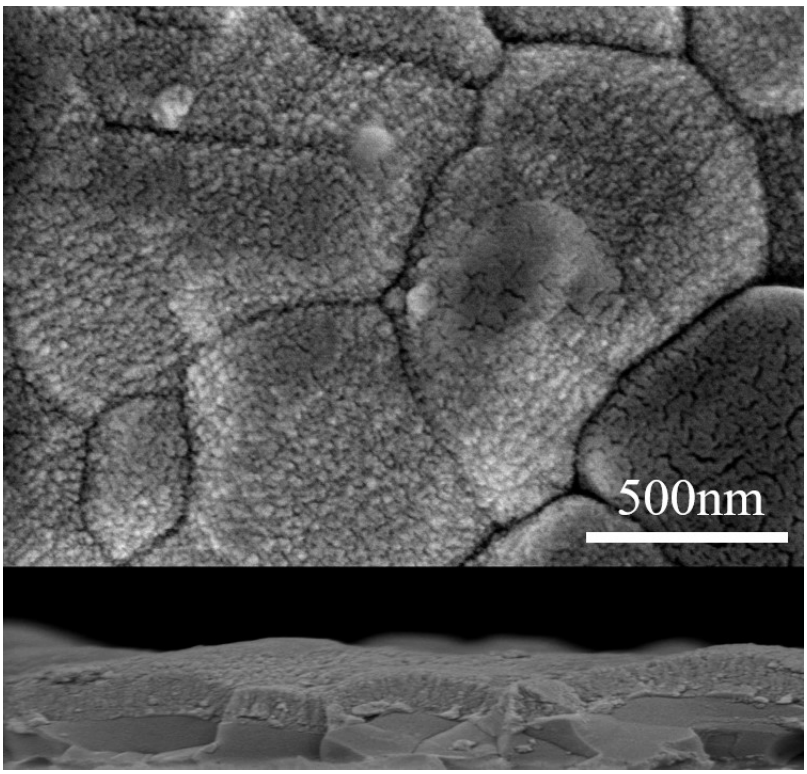

Fig. S7. SEM surface and cross-section morphology of CZTS/CdS.

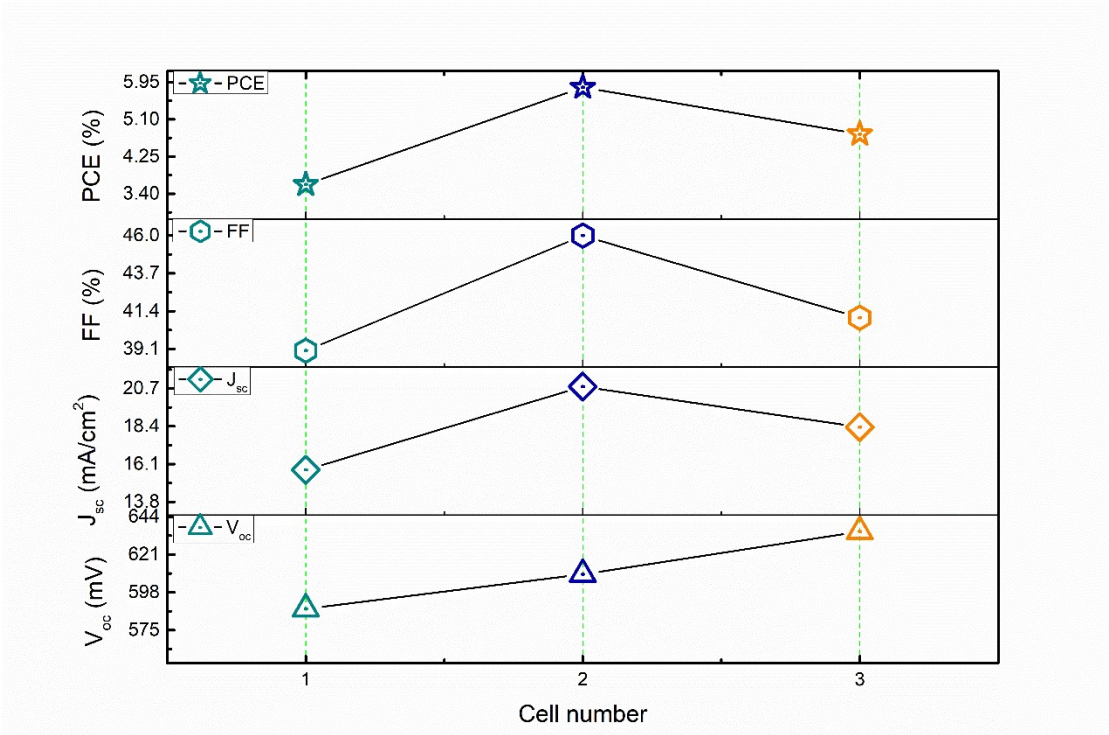

Fig. S8. Variation trend chart of photoelectric parameters of different flexible CZTS solar cells.

In order to obtain statistically significant results, we added performance parameters of 12 solar cells from three groups of samples in the supplemental material. As shown in Table S2, the obtained device performance fluctuates within an acceptable range, and the highest efficiency for each group of samples is shown in the manuscript.

Table S2. Photovoltaic parameters of flexible CZTS thin-film solar cells.

Cell	PCE/%	Voc/mV	Jsc/(mA/cm^2)	FF/%
C1-1	3.61	588	15.75	39
C1-2	3.35	576	15.32	38
C1-3	3.37	580	14.88	39
C1-4	3.52	550	16.01	40
C2-1	5.83	609	20.82	46
C2-2	5.27	612	19.13	45
C2-3	5.46	598	19.86	46
C2-4	5.12	595	19.12	45
C3-1	4.76	635	18.35	41
C3-2	4.31	622	17.36	40
C3-3	4.28	617	16.93	41
C3-4	4.57	630	17.28	42